Supplemental Material: Nucleation in sheared granular matter

Frank Rietz, Charles Radin, Harry L. Swinney, and Matthias Schröter

A. movie-spheres-nucleate-Rietz.avi

The movie shows the nucleation of spheres in the shear cell. For visualization the spheres that are in a crystalline state are shown in a rotating side view. Color indicates the crystal symmetry. At the top right the current state is specified by the global packing fraction, shear cycle, and the number of crystalline spheres. The end of the plateau in the packing fraction is marked by the appearance of the first growing nucleus, which is encircled in the rotating animation and depicted at a constant viewing perspective on the lower right. The wire frame indicates the inner part of the cell, while the green and brown frames are parallel to the shear walls. The bottom of the interrogation volume is cut non-orthogonally because of optical accessibility.

B. Precision of sphere coordinates

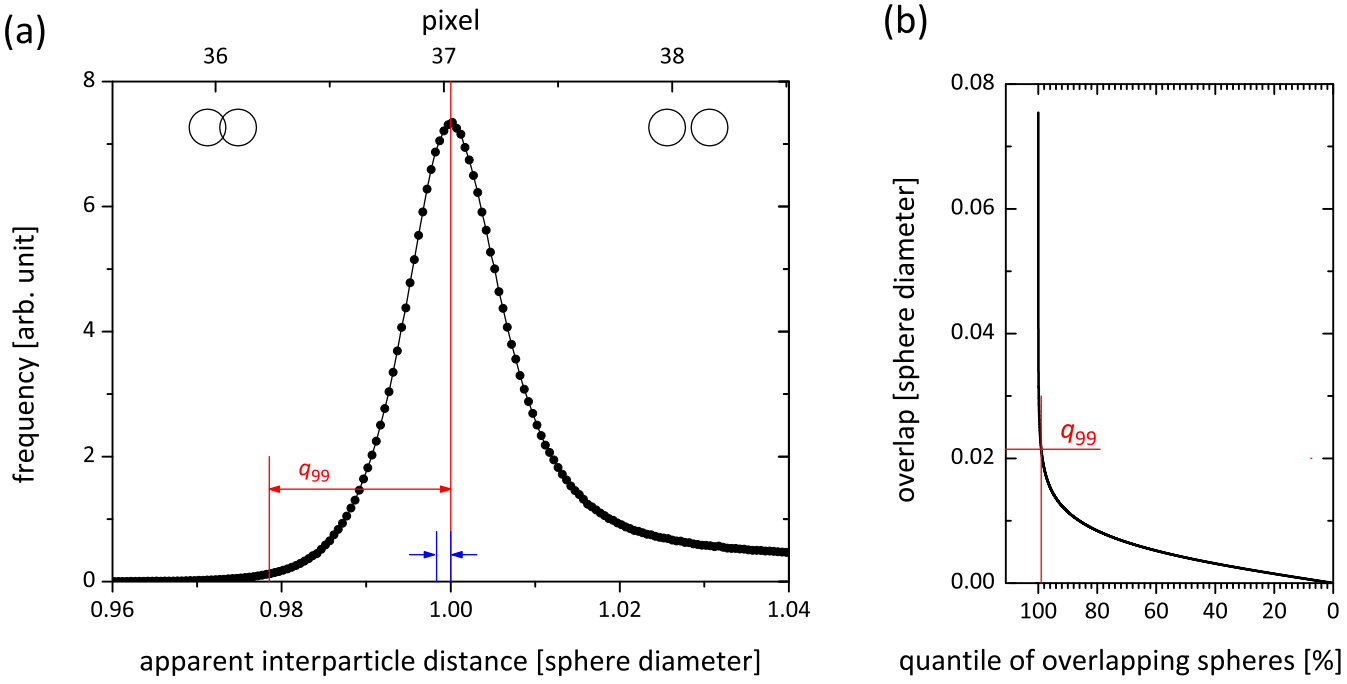

Figure S1. (a) The accuracy of the detected coordinates of the spheres with diameter 3 ± 0.0025 mm is derived from the width of the first peak of the radial distribution function [1]. For ideal monodisperse spheres and known coordinates there would be a step function at a distance of one particle diameter. Under experimental conditions spheres can appear to overlap slightly due to imprecision in the particle positions. The position of the peak maximum of the radial distribution function is used as the mean particle diameter and the width of the left shoulder characterizes the precision of the sphere coordinates. (b) The overlap length for a given percentile of overlapping contacts. Before counting the number of overlaps, spheres are sorted in increasing order, i.e., the smallest overlaps are first. To exclude outliers the width of the left tail in (a) is defined by the largest of the 99% smallest overlaps, the quantile q_{99}. The accuracy of the sphere positions is deduced to be 2% of a diameter. The blue arrows in (a) indicate overlap corresponding to the manufacturer's uncertainty in the diameter of the spheres. The coordinate error due to size tolerance is negligible compared to the inaccuracy of the detection method. The evaluation includes 2.45×10^6 calculated sphere coordinates.

C. Absence of icosahedral symmetry

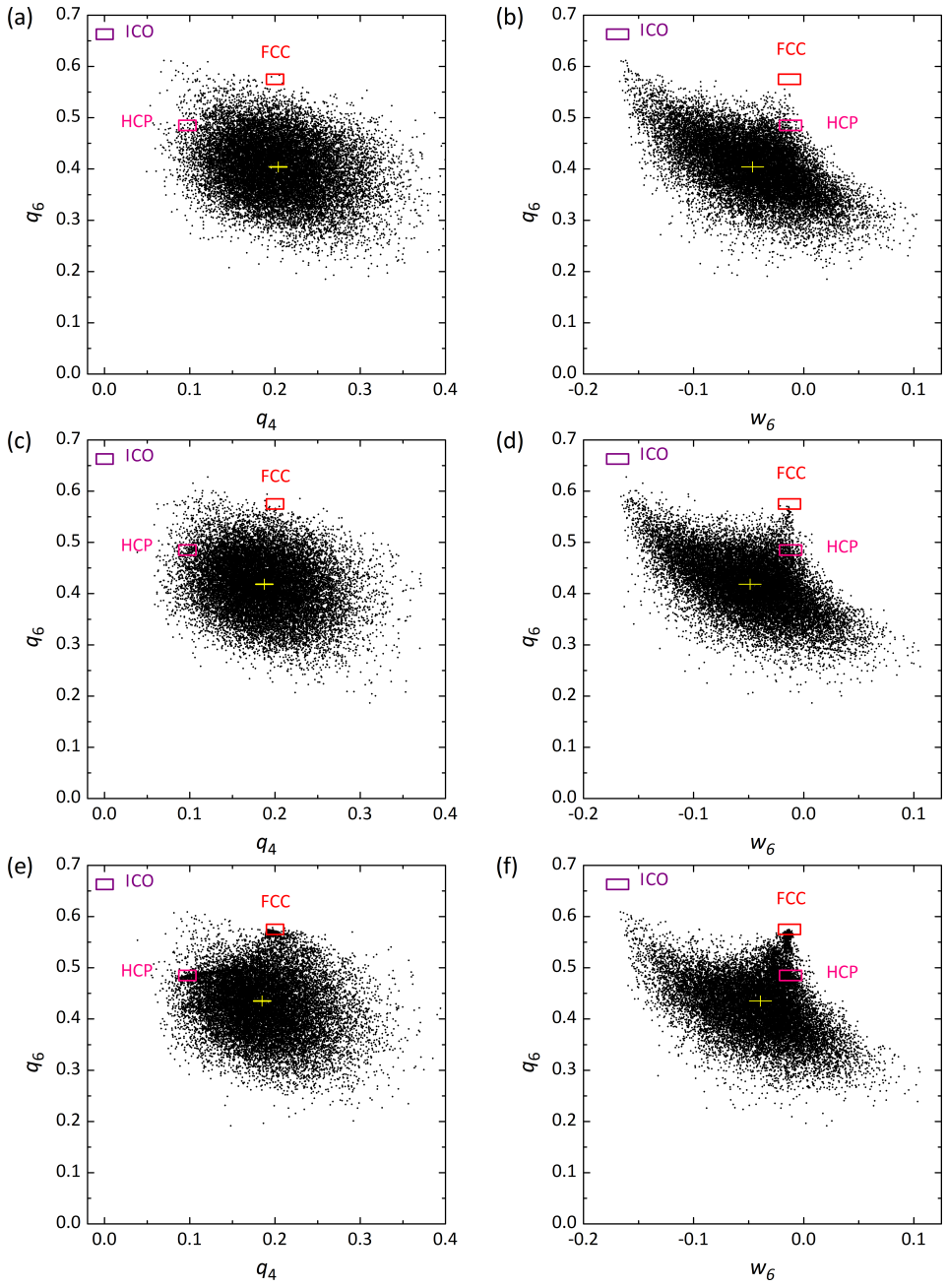

Figure S2. An absence of icosahedral symmetry is indicated by two-dimensional mappings of the order parameters q_6 vs. q_4 and q_6 vs. w_6, where the order parameters q_4, q_6, and w_6 are calculated from the definition in [2] together with the requirement that the Voronoi neighbors are weighted by the areas of their common Voronoi faces [3] (see Fig. S3). Shown are the initial state at $\phi_{global} = 0.627$ (a,b), the phase transition at $\phi_{global} = 0.645$ (c,d) and the final state at $\phi_{global} = 0.654$ (e,f). Values for ideal structures of icosahedral (ICO), face-centered cubic (FCC) and hexagonal close packing (HCP) are located at the centers of the boxes, and the crosses indicate the mean over all spheres in the packing. Using the order parameter values together with a minimum Voronoi density ϕ_{local} (see Fig. S3), we conclude that there is no evidence for icosahedral symmetry, that is, there are no spheres possessing neighbors at the icosahedral positions. This contrasts with the icosahedral ordering that has been found in simulations of frictionless granular spheres [4] and in experiments with deeply cooled colloidal spheres [5].

D. No qualitative influence of different thresholds for crystal classification

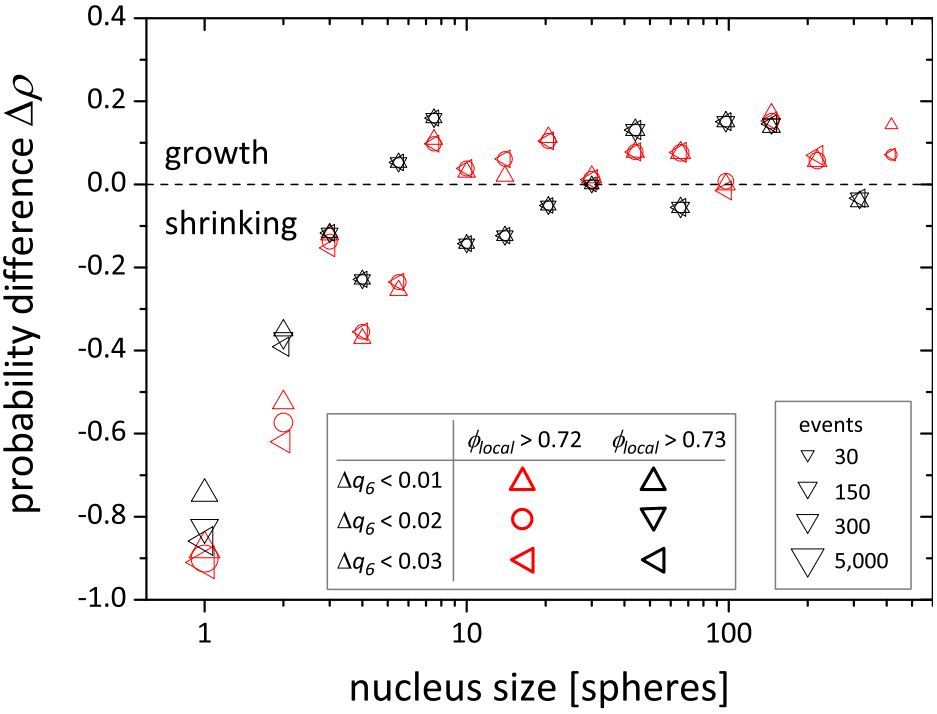

Figure S3. Combinations of different thresholds for Δq_6 and ϕ_{local} do not change the general picture of preferred dissolution of nuclei with fewer than approximately ten spheres. We classify spheres as crystalline if $\phi_{local} > 0.72$ and $\Delta q_6 < 0.02$, i.e., if q_6 is either in the range q_6(FCC)=0.575±0.02 or q_6(HCP)=0.485±0.02 (circle symbol). The rotationally invariant parameter q_6 is used in the literature to characterize the local order of a sphere by considering the relative positions of its surrounding particles [2]. In q_6 neighbors are weighted by the area of the Voronoi faces that they share with the central sphere [3]; thus close neighbors are more influential than distant ones. Symbol size indicates number of observations.

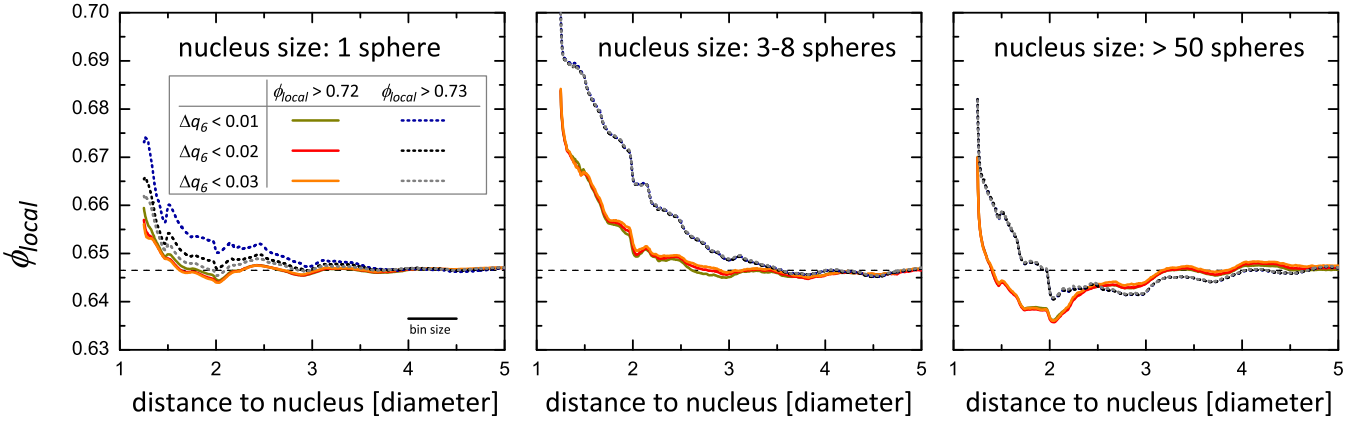

Figure S4. Combinations of different thresholds do not change the general picture of an absence of zones of lower density around subcritical nuclei. The red solid line corresponds to the parameter value used in the paper. To exclude possible interactions between different nuclei, only nuclei separated by at least 6 particle diameters have been included in the analyses here and in Fig. 4(b) and Fig. 4(c), and in Figs. S6, S8, S10, and S12.

E. No qualitative influence of a different crystal definition 1: Geometry of Voronoi cells

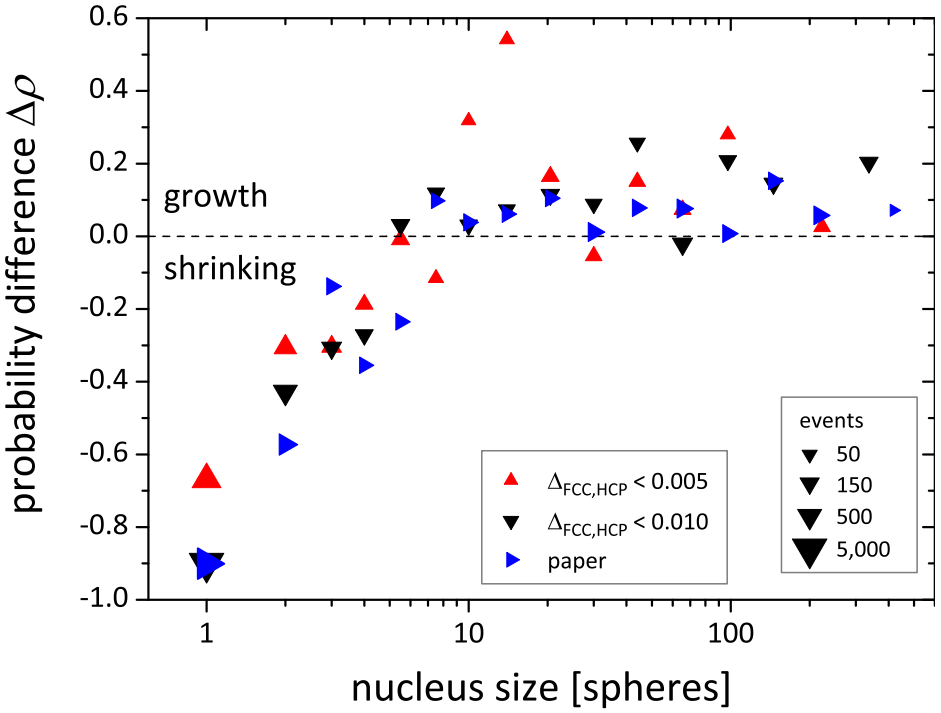

Figure S5. The results obtained for the growth and shrinking rates are insensitive to the definition used for the local crystallinity, whether it is a combination of Δq_6 and ϕ_{local} as in our paper, or it is a rotationally invariant fingerprint calculated from the face normals of a Voronoi cell [6]. A sphere has either FCC or HCP symmetry if the squared difference between the fingerprint of the Voronoi cell and and the fingerprints for ideal FCC or HCP Voronoi cells, $\Delta_{\mathrm{FCC,HCP}}$, is below a threshold, as shown for the two values 0.005 and 0.010. The symbol sizes indicate the number of observations.

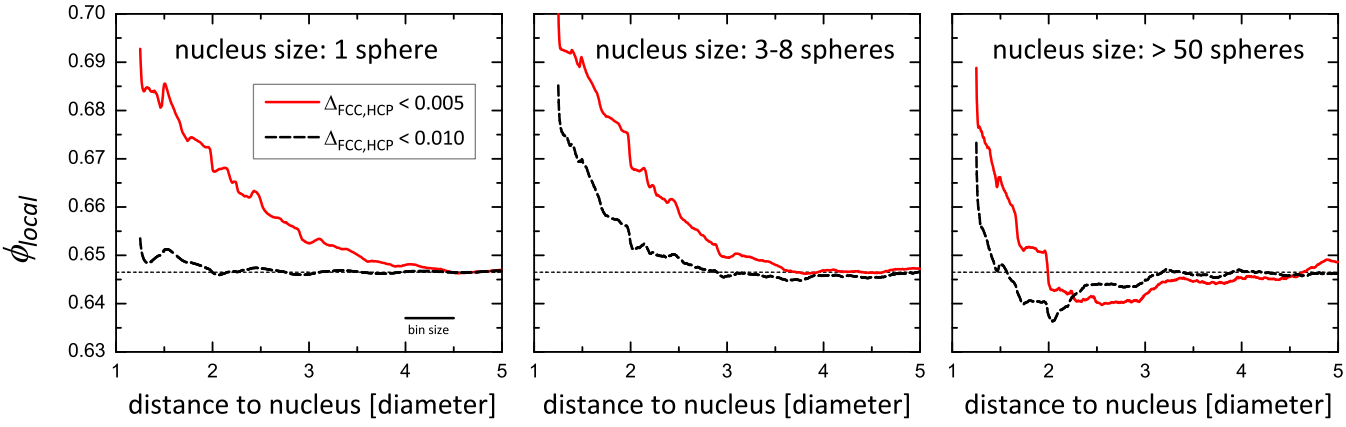

Figure S6. Using $\Delta_{\mathrm{FCC,HCP}}$ as a measure of local order, we find that the local volume fraction dependence on distance from a nucleus is qualitatively similar to that found in Fig. S4. Further, changing the threshold from 1.05 to 1.10 does not make a qualitative change in the properties at the interface.

F. No qualitative influence of a different crystal definition 2: Common neighbor analysis

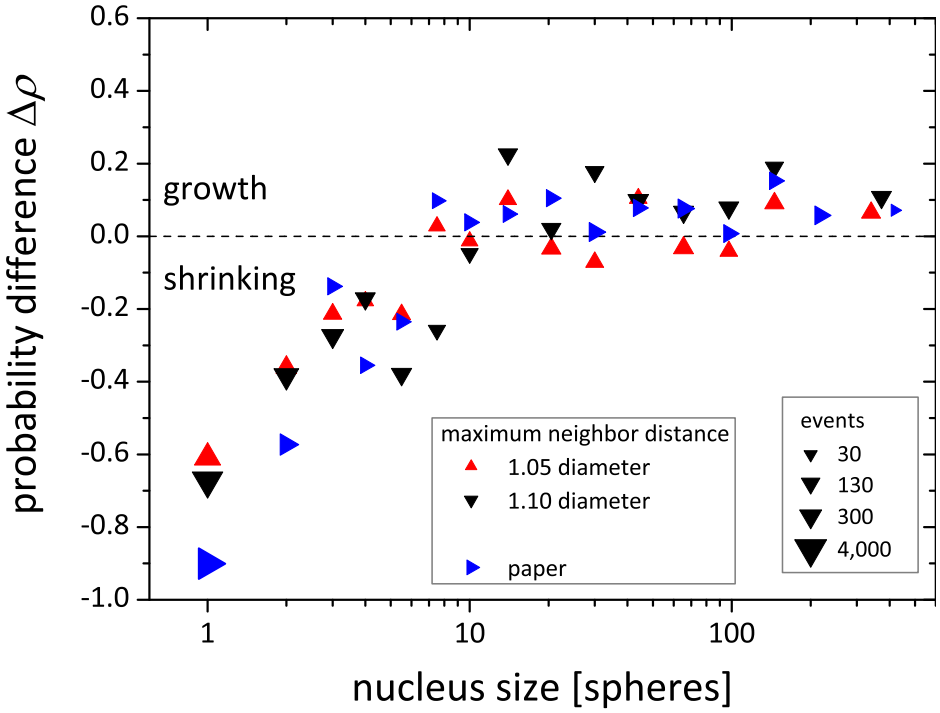

Figure S7. The qualitative picture of the growth rates is unchanged if local crystallinity is detected by a common neighbor analysis [7], which is a widely used tool for structure identification. Among the neighbors a graph is constructed where mutual spheres are checked to determine if they are closer than a maximum distance. For this critical value the intermediate distance of the first and second shells of FCC, HCP, about 1.2 diameter, was suggested [8]. Using the method with this value results in abundant false positive detections; therefore, we use smaller thresholds of 1.05 and 1.10 diameter. A sphere is classified crystalline if the discrete signature derived from the graph is in accord with the signatures of either FCC or HCP. In the version of common neighbor analysis used, spheres with a partly crystalline neighborhood, such as on the surface of a crystallite, are classified as amorphous.

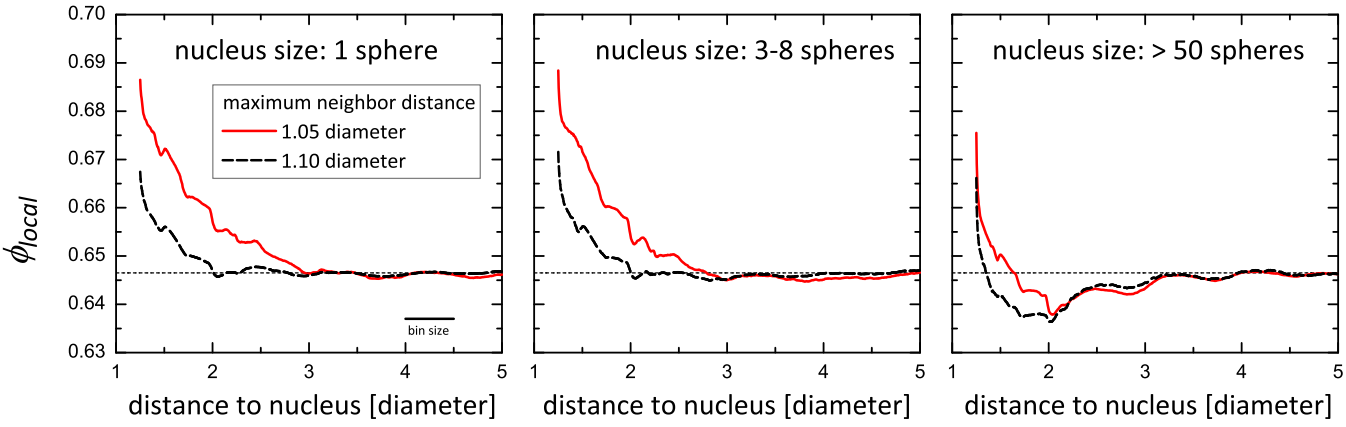

Figure S8. Defining local order by a common neighbor analysis does not make a qualitative change of properties at the nucleus interface.

G. No qualitative influence of a different crystal definition 3: Bond angle analysis

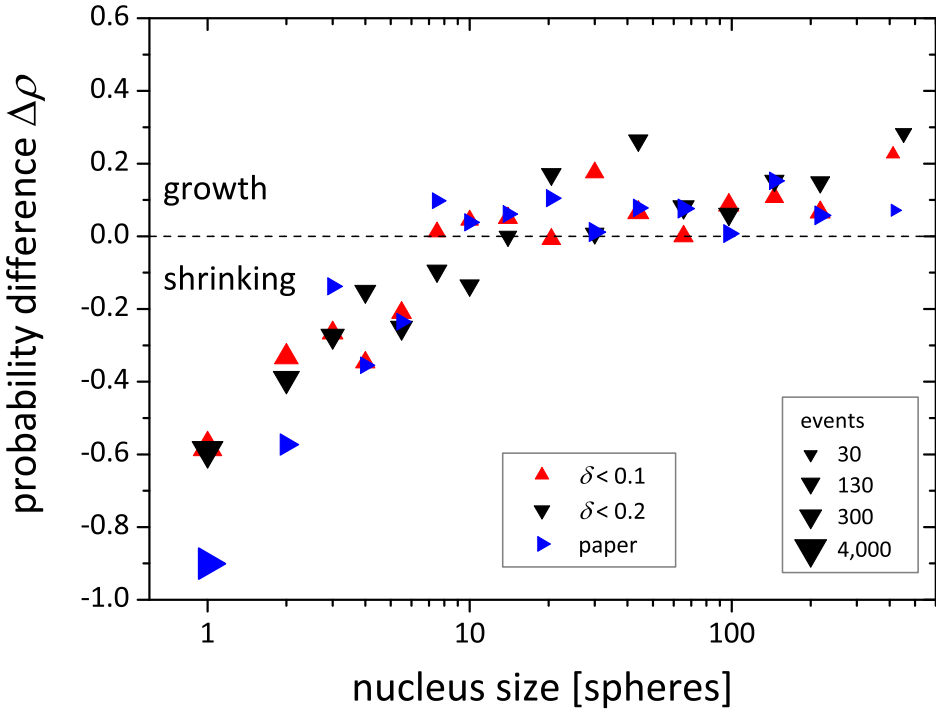

Figure S9. Determination of local crystallinity by another method – bond angle analysis – does not qualitatively change the results for the growth and shrinking of nuclei. Here the angles formed by the central sphere with 2 of the 12 nearest neighbors are compared with the angles for ideal FCC and HCP. If the sum of $\binom{12}{2} = 66$ squared angle differences (for angles in radians) are below the threshold δ, the central sphere is classified as crystalline. Before comparison the angles must be sorted [9].

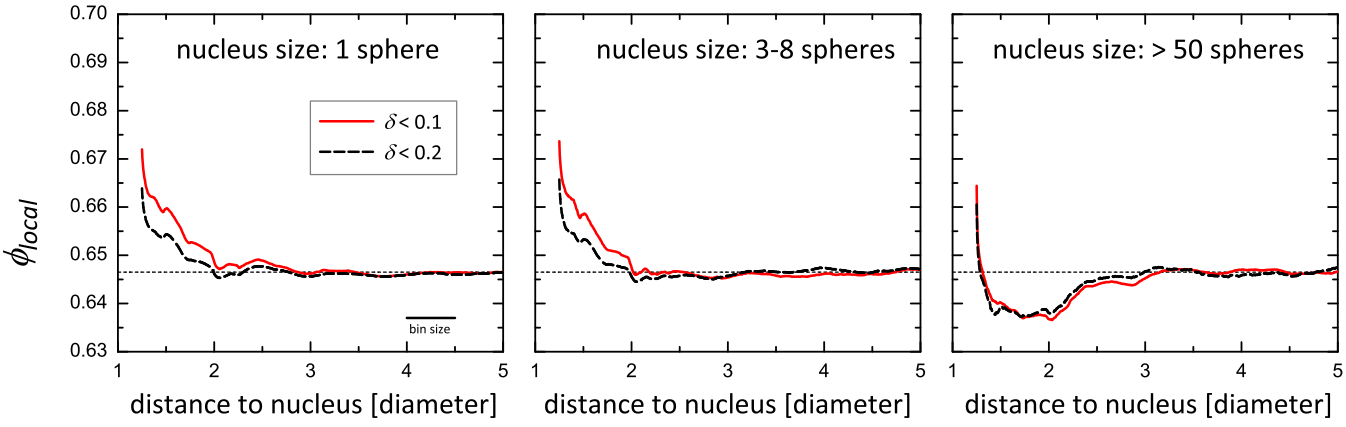

Figure S10. Defining local order by a bond angle analysis does not yield a qualitative change of properties at the nucleus interface.

H. Influence of bin size on interface behavior

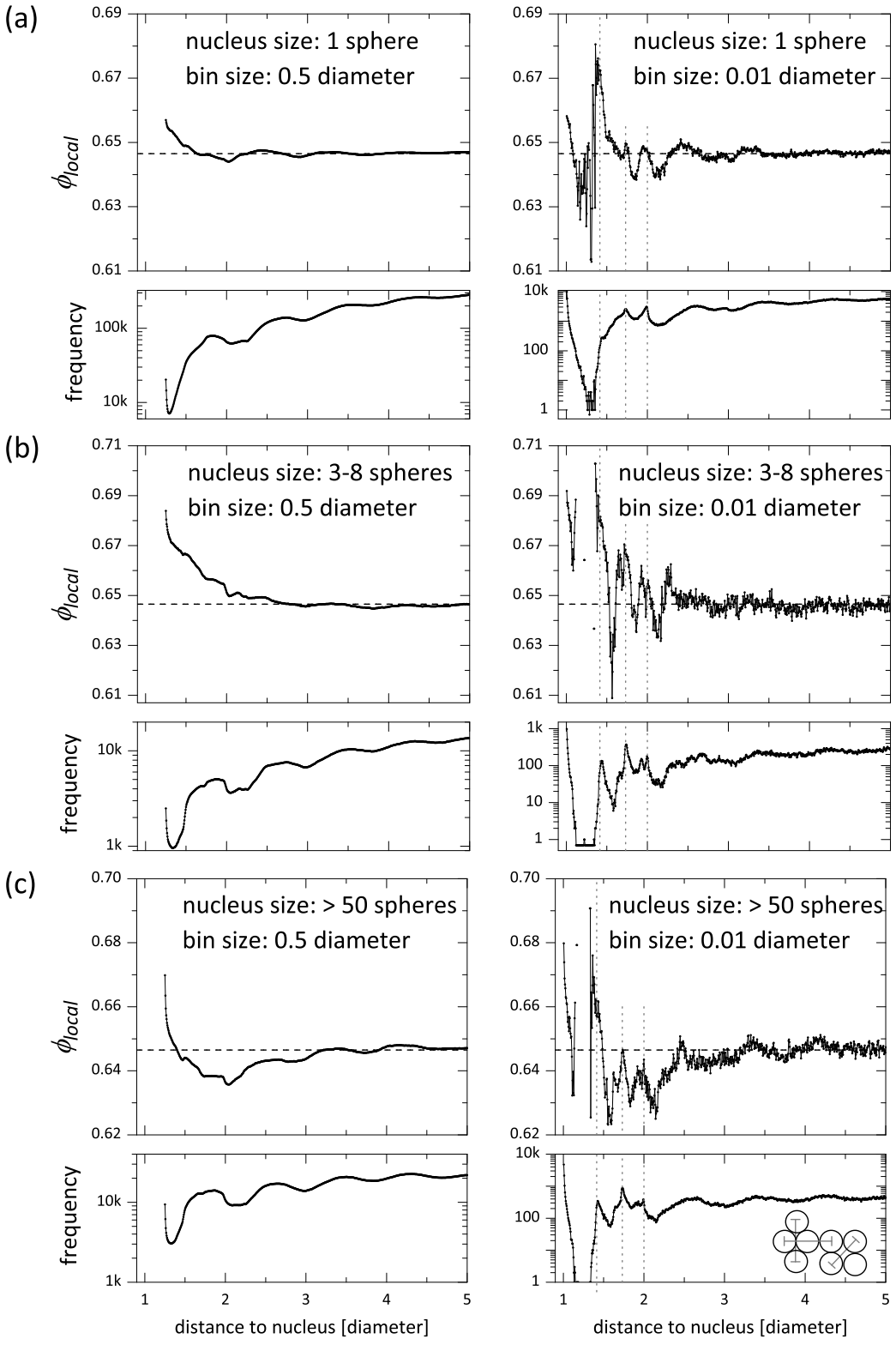

Figure S11. Influence of bin size on ϕ_{local} at the nucleus interface. Left column: bin size 0.5 diameter, as used in the paper; right column: bin size 0.01 diameter. The bin step is always 0.005 diameter. The pronounced peaks in the number densities at $\sqrt{2}$, $\sqrt{3}$, and 2 diameters correspond to the elementary planar distances illustrated on the lower right in (c).

I. No qualitative difference in the comparison of growing and shrinking nuclei

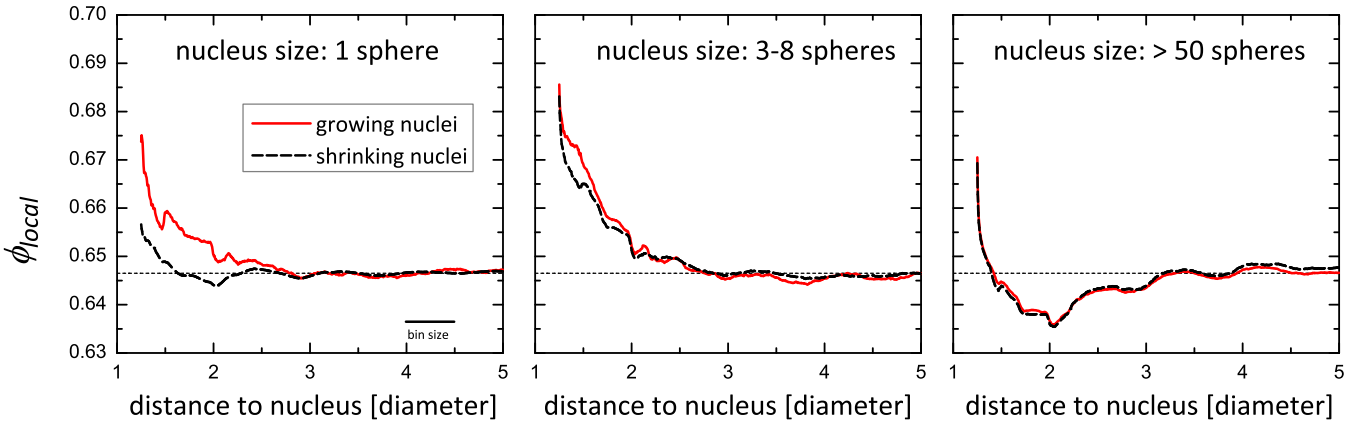

Figure S12. The nuclei are split in groups of growing and shrinking nuclei. There is no qualitative difference in ϕ_{local} at the nucleus interface.

[1] S. Weis and M. Schröter, Rev. Sci. Instrum. **88**, 051809 (2017).
[2] P. J. Steinhardt, D. R. Nelson, and M. Ronchetti, Phys. Rev. B **28**, 784 (1983).
[3] W. Mickel, S. C. Kapfer, G. E. Schröder-Turk, and K. Mecke, J. Chem. Phys. **138**, 044501 (2013).
[4] B. A. Klumov, Y. Jin, and H. A. Makse, J. Phys. Chem. B **118**, 10761 (2014).
[5] M. Leocmach and H. Tanaka, Nat. Comm. **3**, 974 (2012).
[6] S. C. Kapfer, W. Mickel, K. Mecke, G. E. Schröder-Turk, Phys. Rev. E **85**, 030301(R) (2012).
[7] D. Faken and H. Jónsson, Comput. Mater. Sci. **2**, 279 (1994).
[8] A. Stukowski, Modell. Simul. Mater. Sci. Eng. **20**, 045021 (2012).
[9] M. Bargieł and E. M. Tory, Adv. Powder Technol. **12**, 533 (2001).